DOI: http://dx.doi.org/10.1590/2179-10742019v18i41761

Co-Design of a GPS Antenna Low-Noise Amplifier Front-End Circuit

Eduardo S. Sakomura, Diego F. M. Boada, Daniel C. Nascimento
Laboratório de Antenas e Propagação - LAP, Instituto Tecnológico de Aeronáutica
12228-900 São José dos Campos, SP, Brazil
seijis@ita.br, dfmona@yahoo.es, danielcn@ita.br

***Abstract*— This paper presents a clear and fast design procedure for directly matched low noise active integrated microstrip antenna front end circuits. Initially, a theoretical analysis is given for the overall gain equivalence between traditional and directly matched antennas. Then, a detailed procedure is presented for the design and construction of a fully integrated GPS antenna. To validate the proposed procedure, a prototype was built and characterized by measuring the reflection coefficient, radiation pattern, noise figure and the active antenna overall gain. Additionally, a field test comparison was made between the manufactured prototype and a commercially available active antenna using the u-blox NEO-6M GPS receiver module. The prototype experimental and field test results showed excellent performance, thus validating the proposed co-design approach.**

***Index Terms*—** Active integrated antenna, co-design, direct matching, front-end circuit, low noise amplifier, microstrip antenna.

I. INTRODUCTION

In active integrated antennas (AIAs), the miniaturization of wireless telecommunication devices has been a driving factor in the development of new design strategies that depart from the traditional front-end circuit setup [1], [2]. These strategies, usually referred to as co-design or direct matching, get rid of the matching circuitry by directly matching the antenna to the active component, which in turn reduces the size, loss, and complexity of the overall design [3]-[5].

Several prototypes have shown that significant improvements of performance and integrability can be achieved when co-designed antenna-amplifiers are used [6]-[9]. A clear example is shown in [8] where a smaller footprint area was achieved by using a low noise amplifier (LNA) directly matched to the microstrip antenna. Likewise, a microstrip antenna reported in [9] was co-designed in order to meet a given gain matching condition. Amplifying active antennas adopting the co-design strategy showed a significant increase in power added efficiency (PAE) compared to its more traditional counterpart [10], [11].

All of the aforementioned examples presume, without offering theoretical backing, that the traditional front-end circuit – radiator connected to an LNA through a matching network circuit (MNC) – and the co-designed antenna-amplifier are equivalent. Furthermore, most of these works focus on the antenna input impedance (Z_{in}) generation issue rather than the front-end circuit under direct matching conditions design issue.

Brazilian Microwave and Optoelectronics Society-SBMO *received 6 May 2019; for review 9 May 2019; accepted 30 Aug 2019*
Brazilian Society of Electromagnetism-SBMag *ISSN 2179-1074*

DOI: http://dx.doi.org/10.1590/2179-10742019v18i41761

This paper improves on the previously mentioned works by providing a theoretical analysis on the equivalence between the co-designed and traditional front-end circuits. The analytical formulation was derived for receiving systems with active antennas. However, it can also be used for transmitting systems.

Based on said model, a detailed procedure showing all the steps of a front end-circuit project is presented. In this showcase it is used the ATF-34143 transistor [12] to operate in a low noise figure (NF) state. The design is formulated to achieve stability for the particular case in which the impedance $Z_{in} = 81.3 + i38.9\ \Omega$ is generated directly at the LNA input by a microstrip antenna [13].

Experimental and simulation results for reflection coefficient showed excellent agreement. Experimental NF and active gain results showed expected performance, thus validating the proposed design pathway. Finally, a field test comparison is made between the proposed co-designed GPS antenna-LNA prototype and a commercially available AIA, achieving excellent results.

II. THEORY

The design procedure suggested in this paper is based on the overall gain analysis of an antenna connected to the LNA through two different configurations presented in Fig. 1. The first configuration – Fig. 1(a) – is related to the traditional AIA case, where an MNC is used between the antenna and the LNA. The second configuration – Fig. 1(b) – represents the co-designed case, in which the antenna and the LNA are directly matched. It is important to bear in mind that the impedance (Z_{in}) is equal in both setups, given that the LNA used in both configurations is identical.

In the analysis mentioned above, we assumed that both antennas have identical radiation patterns and efficiencies. Under said conditions, according to the equivalent area model [14], the available power (PAV) at their terminals are equal, even for different input impedances ($Z_A \neq Z_{in}$). To satisfy said condition, the specific voltages sources indicated in Fig. 1 must be placed in the antennas' equivalent circuits (red dashed line).

To compare the active gain (antenna + LNA) of both configurations is necessary to calculate the LNA input voltage (V_{LNA}) due to an incident plane wave. First, since the input impedance Z_A of antenna 1 is equal to Z_0 (reference value for the MNC S-parameters) the MNC is admitted lossless and reciprocal, which leads to $S_{22} = \Gamma_{in}$. Provided that the LNAs in Figs. 1(a) and 1(b) are equal, the LNA input voltage magnitude ($|V_{LNA}|$) for both models can be express by the equation below:

$$|V_{LNA}| = V_A \left| \frac{Z_{LNA}}{Z_{LNA} + Z_{in}} \right| \sqrt{\frac{|\mathrm{Re}[Z_{in}]|}{Z_0}} \tag{1}$$

where Z_{LNA} is the amplifier input impedance. This result indicates that the LNA output available power in both configurations are identical, which this in turn means that both circuits present the same active gain.

Brazilian Microwave and Optoelectronics Society-SBMO *received 6 May 2019; for review 9 May 2019; accepted 30 Aug 2019*
Brazilian Society of Electromagnetism-SBMag *ISSN 2179-1074*

DOI: http://dx.doi.org/10.1590/2179-10742019v18i41761

The following conclusions were reached using the analysis mentioned earlier:

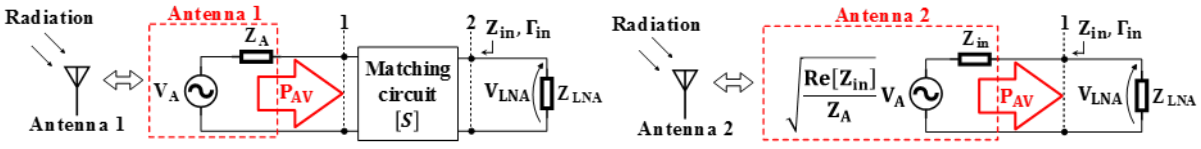

(a) (b)

Fig. 1. Circuital models: (a) LNA matching network - (b) directly matched LNA.

a) The antenna joined to the MNC generating Z_{in} can be replaced by an antenna that generates Z_{in} without affecting the active gain and NF of the overall front-end circuit;
b) An analysis of the amplifier stability is necessary to verify undesired instability caused by the out of band behavior of the antenna impedance;
c) In practical applications the MNC is lossy, resulting in AIAs with lower gains and higher NFs when compared with the directly matched AIAs.

III. METHODS

Following the theoretical analysis, the receiving front-end circuit was designed. The procedure is divided in two stages, RF and DC Bias circuit design, both are detailed in subsequent sections.

A. RF circuit design

Looking for the low noise figure and high gain, the RF circuit was designed using the "Linear Analysis" in the Genesys circuit simulator from Keysight. All dimensions of the distributed components were set for GPS frequency ($f_o = 1.575\ GHz$). The final circuit capable of providing the unconditionally stable LNA condition up to 18 GHz ($K > 1$ and $\Delta < 1$), is presented in Fig. 2. To achieve the above-mentioned condition stabilization methods were applied [15] in conjunction with a technique that adds inductance to the field effect transistor (FET) source [16]. This inductance was identified by manual tuning tool, which is available in the software. Also, it is important to highlight that the design was performed considering the linear operating range, assuring stability and low NF conditions, for output power smaller than 20 dBm (1dB Gain Compression) [12], easily satisfied by the GNSS signal level.

In Fig. 2, the input- and output-matching network provide low NF, high gain, and stabilization for higher frequencies. A circuit capable of decouple RF circuit from DC circuit is highlighted with red dashed line, which are connected through the blue points A and A', depicted in Figs. 2 and 3. Simulated results for gain and NF from the circuit configuration are 15.5 dB and 0.2 dB, respectively.

Since the main purpose of this work is to simplify and improve the performance of a traditional AIAs, the co-design approach was employed. The input matching circuit of an LNA (Fig. 2) is replaced by a CPRMA – Fig. 3(a). The CPRMA and probe to microstrip line transition were simulated

received 6 May 2019; for review 9 May 2019; accepted 30 Aug 2019

ISSN 2179-1074

DOI: http://dx.doi.org/10.1590/2179-10742019v18i41761

and optimized using HFSS. The CPRMA S-parameters results were used as an input to the FET as shown in Fig. 3(a).

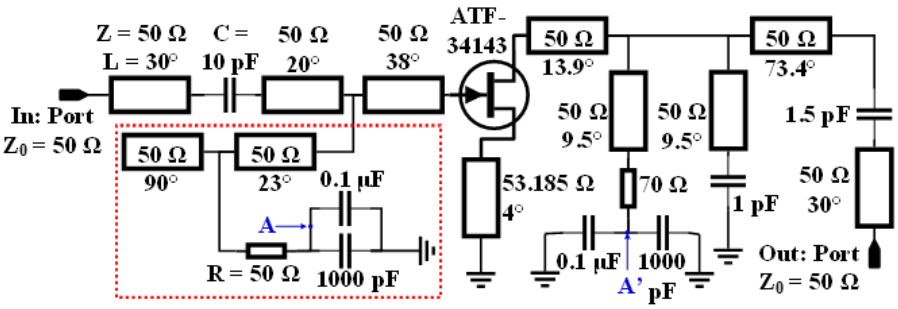

Fig. 2. Schematic of the initial design of the LNA RF circuit.

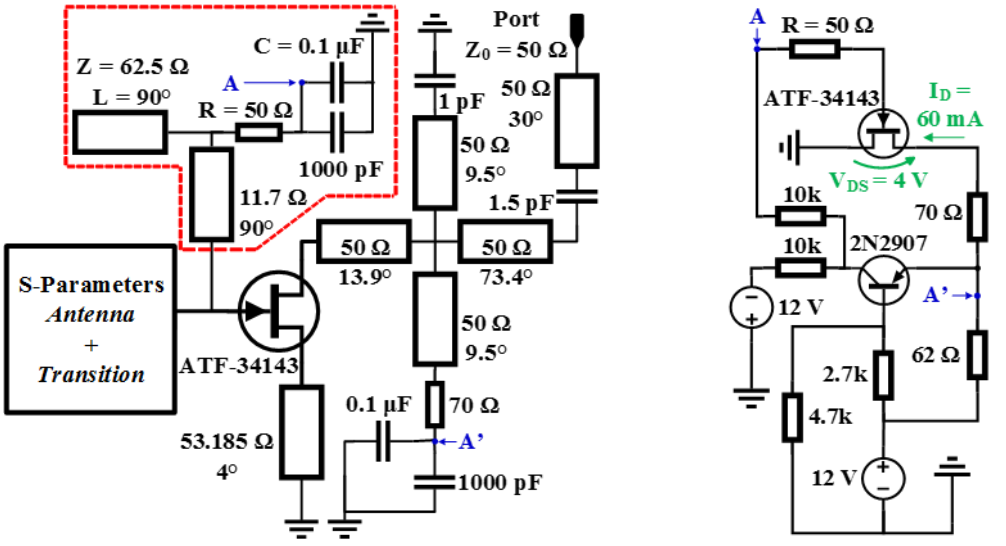

(a) (b)

Fig. 3. Schematic: (a) RF circuit - (b) DC bias circuit.

The main challenge on this circuit is guarantee stability and low NF, which are accomplished by adding a physical microstrip line at FET source. Following [14], the experimental procedure to synthetize the amount of inductance needed from a microstrip line is presented in Section 4.

B. DC bias circuit design

In this project it is chosen an specific S-parameters of ATF-34143 from its datasheet [12], which it is guaranteed when the transistor is biased with $V_{DS} = 4\ V$ and $I_D = 60\ mA$. This condition is defined through the active DC bias circuit [17] – illustrated in Fig. 3(b). This circuit uses a silicon transistor, model 2N2907 PNP, which ensures the required bias as well as a protection of the ATF-34143.

C. Antennas design

To make the measurements presented in Section IV, the matched reference antenna (MRA) and AIA must have identical far field behaviors. Also, in a GPS application the antenna performance is improved using a right-hand circular polarization [18].

received 6 May 2019; for review 9 May 2019; accepted 30 Aug 2019

ISSN 2179-1074

DOI: http://dx.doi.org/10.1590/2179-10742019v18i41761

A probe fed CPRMA was selected for both antennas, allowing the pre-design through a cavity model [19], and then optimized in the electromagnetic solver (HFSS). The antennas' geometries are shown in Figs. 4 and 5, with its main dimensions. The MRA is a traditional antenna with input impedance

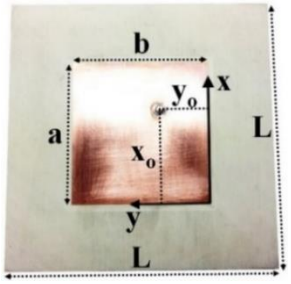

Fig. 4. MRA prototype.

$Z_{MRA} = 50\ \Omega$ at GPS central frequency ($f_o = 1.575\ GHz$). To satisfy the low NF condition the AIA must have $Z_{AIA} = 38.4 + i39.5\ \Omega$ to provide $Z_{in} = 81.3 + i38.9\ \Omega$ in the input of LNA, due to back-to-back configuration [18].

IV. Results and Discussion

In order to reduce the antenna's size, a TMM6 substrate was chosen. Electrical features, final dimensions and probe positions for the prototypes are presented in Table I. From the AIA prototype, presented in Fig. 5, it is possible to see the RF circuit depicted in green, the DC bias circuit in red dashed lines, and also to observe that the antenna probe is, intentionally, positioned close to the transistor, in order to optimize the AIA performance.

A. Stabilization of transistor ATF-34143

For stabilization around f_o an inductive reactance is needed at the FET source, which is accomplished using shorted transmission line. Furthermore, it is important to analyze the antenna input impedance out-of-band behavior and its effects on the stability of the circuit. This can be accomplished by observing the LNA output reflection coefficient (Γ_{out}). A joint circuit/full-wave simulation using the software ANSYS Electronics Desktop was carried out to evaluate Γ_{out} up to 13 GHz, and also the inductance needed at the FET source for optimum performance at f_o. Results for this simulation are presented in Fig. 6.

Due to uncertainty of reference plane in the FET source [16], a shorted line length must be defined experimentally. This was accomplished by progressively incrementing the electrical length of lines L_1 and L_2 (through cutting ΔL with a precision knife) and comparing experimental results with simulated ones. Through this procedure the transmission line electrical length needed to stabilize the circuit can be quickly asserted. After two iterations, the source inductance needed was found. The initial and final configuration are illustrated in Fig. 6.

Brazilian Microwave and Optoelectronics Society-SBMO *received 6 May 2019; for review 9 May 2019; accepted 30 Aug 2019*
Brazilian Society of Electromagnetism-SBMag

ISSN 2179-1074

DOI: http://dx.doi.org/10.1590/2179-10742019v18i41761

B. Measurements

The input impedance of both AIA (without active circuit) and MRA were measured with a network analyzed, model Agilent N5230A, and results are presented in Fig. 7. From Fig. 7(b) is possible to observe that $Z_{AIA} = 38.4 + i39.5\ \Omega$ at f_o, which ensures, after the transition, the Z_{in} required at the LNA input. This impedance is necessary to guarantee the LNA stability and the low NF condition.

TABLE I. ANTENNAS DIMENSIONS AND SUBSTRATE CHARACTERISTICS

Variables	Values		Variables	Values
	AIA	MRA		
a	36.95 mm	37.26 mm	ε_r	6.14
b	35.56 mm	36.09 mm	$\tan\delta$	0.0025
x_0	21.71 mm	24.70 mm	Thickness	1.6 mm
y_0	10.94 mm	13.09 mm	L	7 cm

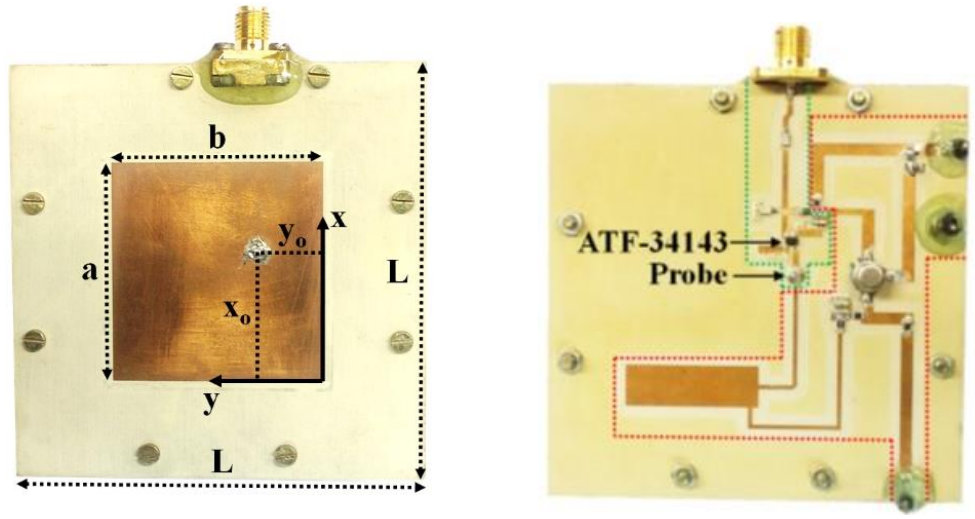

(a) (b)

Fig. 5. Prototype of AIA: (a) bottom view - (b) top view.

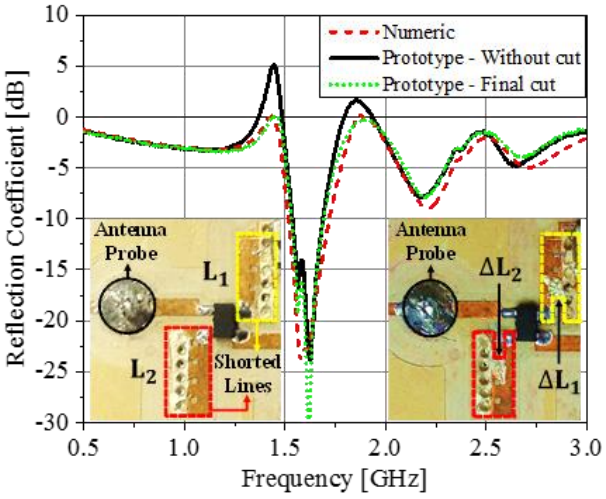

Fig. 6. Numerical vs experimental results of stabilization procedure.

DOI: http://dx.doi.org/10.1590/2179-10742019v18i41761

Broadside axial ratio (AR) and total E-field radiation patterns in the yz-plane of MRA and AIA with the active circuit, were measured in an anechoic chamber and are shown in Fig. 7 and 8. The presented results show that circular polarization was achieved at broadside for both antennas. The minimum measured AR of AIA and MRA was (0.8 dB) located at 1.573 GHz and 1.572 GHz, respectively.

The similarity between radiation patterns of AIA and MRA is required for the LNAs characterization [20], which is corroborated by the good agreement between simulation and experimental results. A slight difference between the AIA radiation pattern measurement and the simulated pattern [Fig. 8(b)] occurs mainly in the back lobe. This difference is mainly due to the scattering from the active circuit on the back of the AIA and the coaxial cable, which are not computed in the electromagnetic simulations.

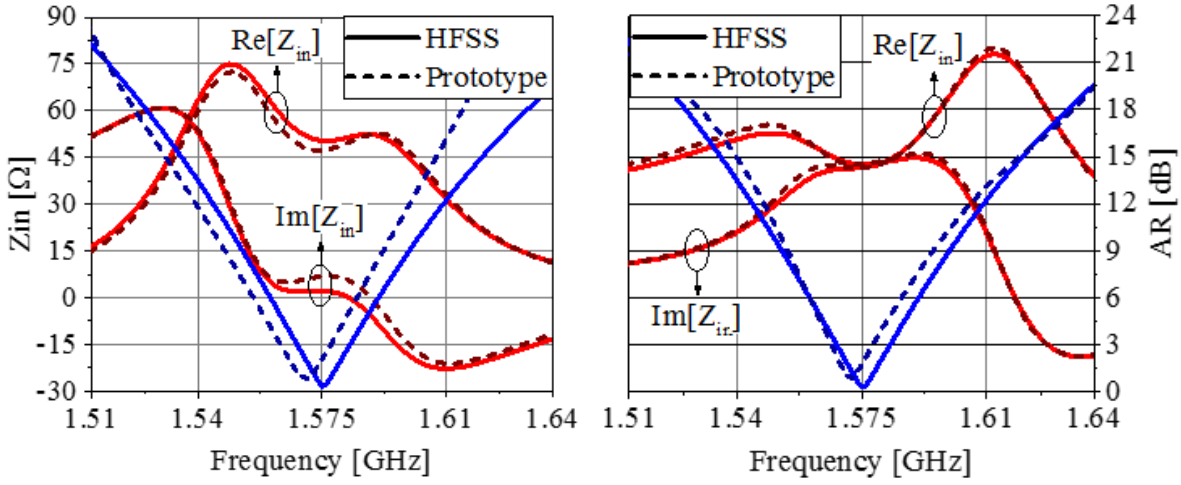

(a) (b)

Fig. 7. Simulated and experimental results: (a) MRA - (b) AIA.

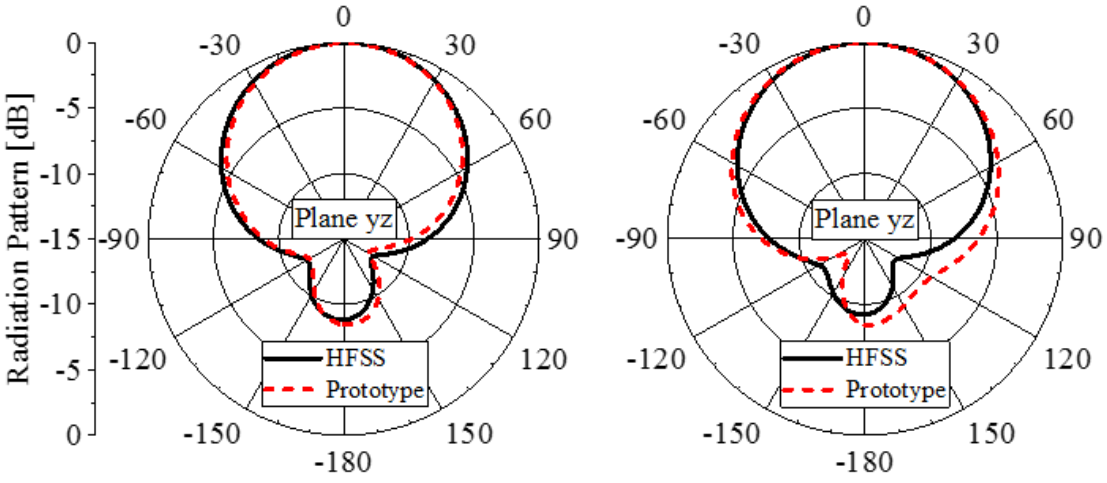

(a) (b)

Fig 8. Simulated and experimental normalized total E field: (a) MRA - (b) AIA.

A signal analyzer (SA), model Keysight CXA N9000B, was used to measure NF and gain. The NF was measured following the procedure in [20], and its experimental setup is showed in Fig. 9. A

ISSN 2179-1074

DOI: http://dx.doi.org/10.1590/2179-10742019v18i41761

summary of the measures is described in the flow chart presented in Fig. 10. The LNA gain (G_{LNA}) and NF calculated were 15 *dB* and 0.7 *dB*, respectively.

C. Field test performance using a GPS receiver

The AIA prototype was field-tested and compared to a low-cost commercial AIA to assess its performance. In this process, the Carrier-to-Noise ratio (C/No) [21] and positioning estimation were evaluated using a GPS module receiver u-blox NEO-6M.

Using the GPS receiver, the average values of current position, number of viewed satellites and C/No level per satellites were recorded for both the proposed prototype and commercial antenna. Measurements for both AIAs, presented in Table II, were performed under the following experimental conditions:

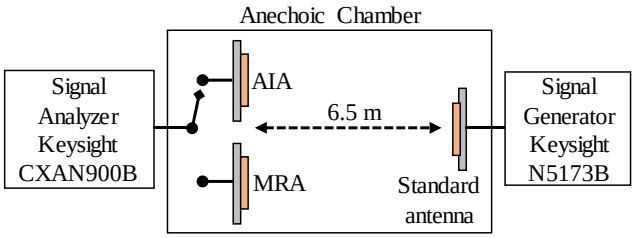

Fig. 9. Experimental setup for gain measurement.

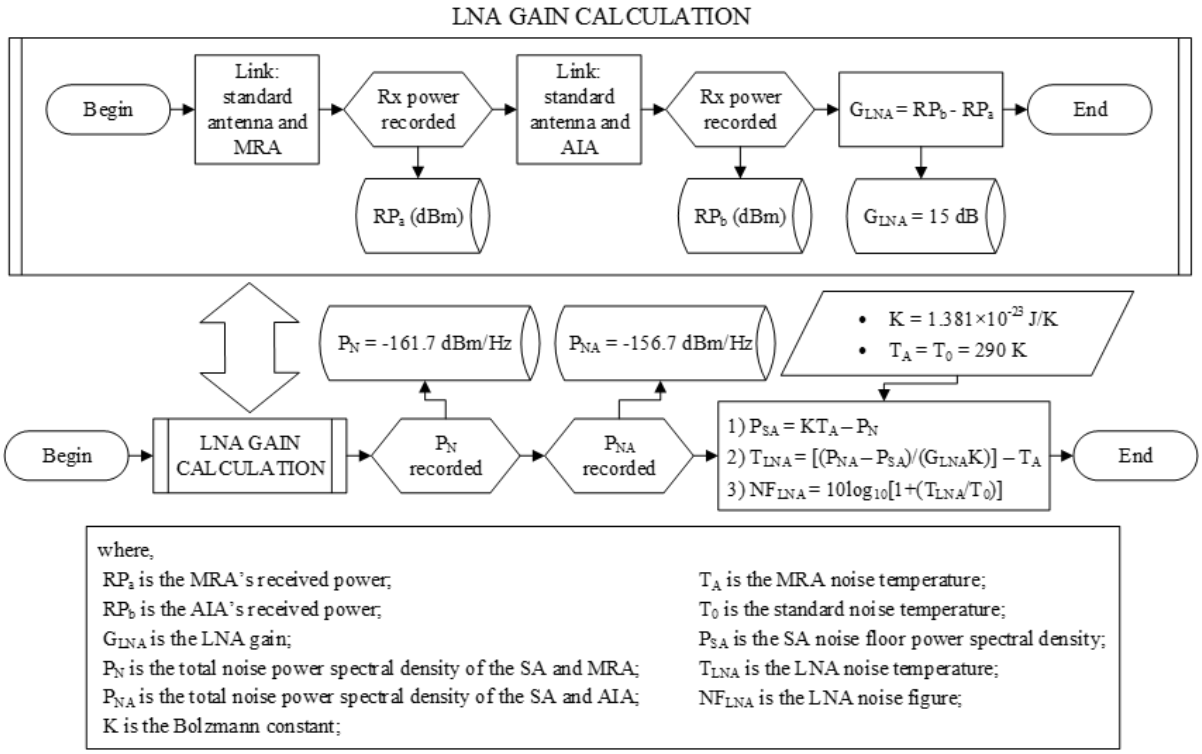

Fig 10. Flow chart describing the measures of LNA gain and NF.

  ISSN 2179-1074

DOI: http://dx.doi.org/10.1590/2179-10742019v18i41761

TABLE II. MEASUREMENTS (POSITION, NUMBER OF SATELLITES AND C/No) OF PROTOTYPE AND COMMERCIAL ANTENNA

Antenna	**Position**		**Difference** ($\|Position_{Google} - Position_{Measure}\|$)		**Number of satellites**	**C/No [dB-Hz]**
	Latitude	**Longitude**	**Latitude**	**Longitude**		
Prototype	23°12'32.4"S	45°52'30.4"W	3"S	–	6	27.2
Commercial	23°12'32.5"S	45°52'29.9"W	2"S	5"W	5	23.8

- Geographical position: Laboratory of Antenna and Propagation (LAP) (23°12'32.7"S 45°52'30.4"W taken from Google Maps);
- Amount of time: 8 hours for 5 days;
- Identical environmental conditions since the measurements of both antennas were simultaneous.

V. CONCLUSIONS

In this paper a methodology was presented to fully design and characterize a co-designed microstrip antenna-LNA for GPS applications. The main purpose was to design an LNA directly connected to a CPRMA, and said antenna operates simultaneously as a radiator and matching circuit. The overall gain of the co-designed and conventional AIA was discussed through a theoretical analysis which verified the equivalence between them. Said theoretical backing provides designers with a more comprehensive understanding of directly matched AIA.

Using joint circuit/full-wave simulations and experimental results, an optimal performance was attained from the transistor, proving that direct matching is a good approach to save space without degrading NF and gain performance. Field-test results showed that the AIA prototype presented better average values of C/No level and number of viewed satellites than the commercial AIA.

In commercial applications, the GNSS receiver usually has an LNA in the first stage and also provides a DC voltage level at RF port [22]-[23] for an active antenna. Consequently, the use of the proposed AIA requires paying attention to the setup. For example, a DC block can be introduced between the active antenna and receiver to avoid an undesired DC coupling between them. Otherwise, the active circuit of the antenna can be modified to comply with the technology of a specific receiver.

The project complexity of the proposed and commercial solutions are pretty much the same. However, the proposed design provides some advantages related to size and loss reduction, and therefore a better noise figure. The costs to fabricate the proposed antenna is mainly related to the cost of the dielectric substrate, LNA, and the chosen manufacturing process, which makes it equivalent to the commercial one. Consequently, it is concluded that the proposed design technique is a powerful, efficient, and feasible approach for an AIA.

ACKNOWLEDGMENT

The authors would like to thank CNPq for sponsoring Projects 166603/2017-1 and 305425/2018-8.

  ISSN 2179-1074

DOI: http://dx.doi.org/10.1590/2179-10742019v18i41761

REFERENCES

[1] M. Sharawi, F. Ghannouchi, S. Dhar and O. Hammi, "Miniaturized active integrated antennas: a co-design approach", *IET Microwaves, Antennas & Propagation*, vol. 10, no. 8, pp. 871-879, 2016.

[2] J. Anguera, A. Andújar, M.C. Huynh, C. Orlenius, C. Picher, and C. Puente, "Advances in Antenna Technology for Wireless Handheld Devices", *International Journal on Antennas and Propagation*, vol. 2013, Article ID 838364.

[3] A. Pal, H. Zhou, A. Mehta, E. Nagasundaram, J. Lees, and D. Mirshekar-Syahkal, "Co-design of an Antenna-Power Amplifier RF Front-end Block Without Matching Network for 2.4 GHz Wi-Fi Application", *IEEE Radio and Wireless Symposium (RWS)*, 2017.

[4] X. Qing, C. K. Goh and Z. N. Chen, "Impedance Characterization of RFID Tag Antennas and Application in Tag Co-Design", *IEEE Transactions on Microwave Theory and Techniques*, vol. 57, no. 5, pp. 1268-1274, 2009.

[5] A. Dierck, F. Declercq and H. Rogier, "Review of active textile antenna co-design and optimization strategies," *2011 IEEE International Conference on RFID-Technologies and Applications*, 2011.

[6] S. Gao, Y. Qin and A. Sambell, "Circularly polarized broadband high-efficiency active integrated antenna," *Microwave and Optical Technology Letters*, vol. 48, no. 11, pp. 2145-2148, 2006.

[7] K. Eccleston, "Four FET active integrated microstrip antenna," *Microwave and Optical Technology Letters*, vol. 51, no. 12, pp. 2997-3000, 2009.

[8] R. Raj, S. Kundukulam, C. Aanandan, K. Vasudevan, P. Mohanan and P. Kumar, "Compact amplifier integrated microstrip antenna," *Microwave and Optical Technology Letters*, vol. 40, no. 4, pp. 296-298, 2004.

[9] A. Kaya and S. Çömlekçi, "The design and performance analysis of integrated amplifier patch antenna," *Microwave and Optical Technology Letters*, vol. 50, no. 10, pp. 2732-2736, 2008.

[10] H. Kim, I-J. Yoon and Y. J. Yoon, "A novel fully integrated transmitter front-end with high power-added efficiency," *IEEE Transactions on Microwave Theory and Techniques*, vol. 53, no. 10, pp. 3206-3214, 2005.

[11] J. Lee, C. Wu and T. Itoh, "A power efficient active integrated antenna," *Microwave and Optical Technology Letters*, vol. 55, no. 6, pp. 1240-1243, 2013.

[12] Avago Technology, "Broadcom Limited," [Online]. Available: https://www.broadcom.com/products/wireless/transistors/fet/atf-34143.

[13] D. Moná, E. Sakomura and D. Nascimento, "Circularly polarised rectangular microstrip antenna design with arbitrary input impedance," *IET Microwaves, Antennas & Propagation*, vol. 12, no. 9, pp. 1532-1540, 2018.

[14] C. Balanis, *Antenna theory*. Hoboken: Wiley-Interscience, 2005.

[15] G. González, *Microwave transistor amplifiers*. Upper Saddle River: Prentice Hall, 1997.

[16] Avago Technology, "Broadcom Limited," [Online]. Available: https://www.broadcom.com/products/wireless/transistors/fet/atf-34143#documentation.

[17] Agilent Technologies, "Hewlet Packard Woodshot," [Online]. Available: http://www.hp.woodshot.com/hprfhelp/products/xrs/atf10xxx.htm#aps_lit.

[18] D. Mona, E. Sakomura and D. Nascimento, "Microstrip-to-Probe Fed Microstrip Antenna Transition," *2018 IEEE International Symposium on Antennas and Propagation & USNC/URSI National Radio Science Meeting*, 2018.

[19] F, Lumini, L. Cividanes and J. d. S. Lacava. "Computer aided design algorithm for singly fed circularly polarized rectangular microstrip patch antennas", *RF and Microwave Computer-Aided Engineering*, vol. 9, no. 1, pp. 32-41, 1999.

[20] H. An, B. Nauwelaers, and A. van de Capelle, "Noise figure measurement of receiving active microstrip antennas", *Electron. Lett.*, vol. 29, no. 18, pp. 1594–1596, Sept. 1993.

[21] M. Sharawi and D. Aloi, "WLC26-6: C/No Estimation in a GPS Software Receiver in the Presence of RF Interference Mitigation via Null Steering for the Multipath Limiting Antenna", *IEEE Globecom 2006*, 2006.

[22] U-blox, "NEO-6 u-blox 6 GPS Modules," [Online]. Available: https://www.u-blox.com/sites/default/files/products/documents/NEO-6_DataSheet_%28GPS.G6-HW-09005%29.pdf.

[23] Great Scott Gadgets, "HackRF One," [Online]. Available: https://greatscottgadgets.com/hackrf/one/.

